Maejo Int. J. Sci. Technol. **2011**, *5*(01), 47-57

Maejo International Journal of Science and Technology

ISSN 1905-7873
Available online at www.mijst.mju.ac.th

Full Paper

Hybrid QM/MM study on the deglycosylation step of chitin hydrolysis catalysed by chitinase B from *Serratia marcescens*

Jitrayut Jitonnom [1], Adrian J. Mulholland [2], Piyarat Nimmanpipug [1, 3] and Vannajan S. Lee [1, 3, *]

[1] Computational Simulation and Modelling Laboratory (CSML), Department of Chemistry and Centre for Innovation in Chemistry, Chiang Mai University, Chiang Mai, 50200, Thailand
[2] Centre for Computational Chemistry, School of Chemistry, University of Bristol, Bristol BS8 1TS, UK
[3] Thailand Centre of Excellence in Physics, CHE, 328 Su Ayutthaya Road, Bangkok, 10400, Thailand
* Corresponding author, E-mail: vannajan@gmail.com; Tel. +6653943341 ext. 117; Fax +6653892277

Received: 11 October 2010 / Accepted: 13 February 2011 / Published: 15 February 2011

Abstract: Chitinase B (ChiB) from *Serratia marcescens* is an exo-chitinase that degrades chitin chains from the non-reducing end by cleaving off a dimer or trimer sugar product. This enzyme features the substrate-assisted mechanism for the cleavage of the β-1,4-glycosidic bond. In this study, the deglycosylation step of chitin hydrolysis catalysed by *S. marcescens* ChiB is investigated by hybrid QM/MM method. Potential energy surface calculated at AM1/CHARMM22 level shows the presence of two transition states (TS1 and TS2) indicating that the deglycosylation path follows a stepwise mechanism in which the nucleophilic attack of catalytic water at the anomeric carbon occurs as the first step followed by proton abstraction. The calculated potential energy barriers for TS1 and TS2 are 26.8 and 4.0 kcal/mol, suggesting that the nucleophilic attack by water molecule is the rate-limiting step for the deglycosylation. In addition, an oxocarbenium-like character in TS1 can also be captured.

Keywords: chitinase B, *Serratia marcescens*, QM/MM, enzyme catalysis, glycoside hydrolase

Maejo Int. J. Sci. Technol. **2011**, *5*(01), 47-57

INTRODUCTION

Chitinase B (ChiB) (EC 3.2.1.14) belonging to a member of glycoside hydrolase (GH) family 18 [1-2] effects the hydrolysis of chitin, a linear insoluble polymer of N-acetylglucosamine (GlcNAc or NAG), which is believed to be the second most abundant polysaccharide on earth after cellulose. This enzyme has received much attention as an attractive target for development of new drugs/inhibitors [3] with chemotherapeutic potential against fungi, insects and malaria transmission or anti-inflammatory potential against asthma and allergic diseases. Designing such inhibitors with sufficiently high selectivity and affinity requires a detailed understanding of the catalytic mechanism at the molecular level.

Catalysis by ChiB from *Serratia marcescens* has been proposed to involve a substrate-assisted double displacement which leads to the retention of configuration at the anomeric carbon [4-6]. The overall reaction of ChiB proceeds in two main steps, i.e. glycosylation and deglycosylation. Two key catalytic residues (Asp142 and Glu144) were identified previously by both structural and kinetic studies to play an important role in catalysis by ChiB [4, 6-7]. In the glycosylation step, Asp142 assists in the formation of an oxazolinium ion intermediate by polarising the 2-acetamido group of the substrate to increase its nucleophilicity, thereby promoting attack of the carbonyl oxygen (O7) at the anomeric centre (C1). Glu144 meanwhile acts as a general acid, encouraging departure of the aglycon leaving group [8] by means of proton transfer from Glu144. In the deglycosylation step (Figure 1), the oxazolinium intermediate is broken down in a reverse manner to the glycosylation step: Glu144 is believed to act as a general base, promoting attack of a water molecule at the anomeric center (C1), while Asp142 is thought to facilitate the expulsion of the 2-acetamido group from the anomeric centre (C1), yielding a sugar hemiacetal product with overall retention of stereochemistry.

Hybrid or combined QM/MM (quantum mechanics/molecular mechanics) approach, introduced to enzyme reactions by Warshel and Levitt [9], treats the central reacting system with a quantum chemical method while representing the remainder of the system by a classical empirical force field model. This technique has an advantage not only of verifying a proposed reaction mechanism, but also of elucidating a transition state or intermediate, a performance that may not be achievable by experimental methods. Application of this technique to the study of an enzymatic reaction has increased significantly over the past two decades [10-11]. For the GH enzymes, this QM/MM technique has increasingly been applied and has provided new insights into the hydrolysis of glycosidic bonds, as evidenced by recent QM/MM studies on various enzymes such as lysozyme [12], endoglucanase [13], β-galactosidase [14], cellulase [15] and Golgi α-mannosidase [16]. However, thus far no work has been reported on the QM/MM study of the ChiB-assisted hydrolysis mechanism. Very recently, our group [17] has studied the glycosylation step by *S. marcescens* ChiB by using the combined QM/MM method. Here, we aim to continue our previous QM/MM study in order to fully understand the overall action of ChiB.

In this study, the hydrolysis of oxazolinium ion intermediate (deglycosylation step) by *S. marcescens* ChiB is investigated in detail by using hybrid QM/MM calculations. The QM/MM potential energy surface calculated at AM1/CHARMM22 level is carried out to track a possible reaction pathway and locate and characterise the structures corresponding to the stationary points in

Maejo Int. J. Sci. Technol. **2011**, *5*(01), 47-57

the deglycosylation path, thus giving important insights into the mechanism of deglycosylation reaction of chitin catalysed by *S. marcescens* ChiB.

METHODS

Model Preparation

The starting model of the ChiB-intermediate complex in the deglycosylation step was built on the basis of X-ray crystallographic structure PDB codes [6] of 1E6R and 1E6Z for the *S. marcescens* ChiB complexed with the allosamidin inhibitor and its reaction intermediate respectively. These two crystal structures were superimposed by using chain A of 1E6Z as a template to generate the ChiB-intermediate model structure containing a dimeric product (NAG_2 at subsite –1, –2) and a leaving group of dimeric sugar (NAG_2 at subsite +1, +2) as shown in Figure 4. These subsite numbers indicate the sugar binding subsite of NAG_5 (–2 to +3) [6]. The observed catalytic water molecule and other crystallographic water molecules were kept. Hydrogen atoms were added using HBUILD module in CHARMM [18] with all residues in their physiological protonation state. The only exception was the acid/base residue (Glu144), which was deprotonated in the second step as proposed by van Aalten et al. [6] while the Asp142 residue remained protonated.

QM/MM MD Simulation

In QM/MM MD simulation, the system was partitioned into QM and MM regions. The QM region consisted of the putative oxazolinium ion intermediate, one catalytic water molecule and side-chain groups of Asp142 and Glu144, leading to a total of 46 atoms (Figure 1). These QM residues were treated with AM1 semi-empirical method [19], which has been shown to satisfactorily describe the first step of ChiB-assisted reaction [17]. Three bonds crossing the QM/MM boundary were capped with the 'QQ link atoms' (Figure 1). The charge on the QM system was neutral. Other protein (5871), water (1650) and sugar atoms (131) were treated using the modified version of all-atom CHARMM22 MM force field [20]. The simulations employed a stochastic boundary approach [21]. The system was solvated by superimposing a 25-Å-radius sphere of TIP3P water molecules centred on the anomeric C1 carbon and equilibrated for 1.6 ns of CHARMM QM/MM molecular dynamics (MD) by a procedure similar to that of Lodola et al. [22]. MD snapshots were chosen for subsequent restrained QM/MM minimisation with adopted-basis Newton-Raphson method until the gradient was less than 0.01 kcal/(mol•Å). The resulting minimised structures were selected as starting point for reaction path calculation. The simulation was carried out with CHARMM version 27b2 [18].

Reaction Path Calculation

The two-dimensional (2D) potential energy surface (PES) of a reaction path was determined by adiabatic mapping calculation using CHARMM's RESDistance facility [18]. The reaction was described by two discrete coordinates (R_X and R_Y) to represent the two key individual steps of the deglycosylation. As illustrated in Figure 1, a proton (H_w) is abstracted from the catalytic water molecule by Glu144 (event ***Y***), which is described by $R_Y = r[O_w,H_w] - r[O\varepsilon_1,H_w]$. After that the

Maejo Int. J. Sci. Technol. **2011**, *5*(01), 47-57

deprotonated water attacks the anomeric C1 carbon, resulting in a collapse of the oxazolinium ion intermediate (event ***X***), which is described by $R_X = r[C1,O7] - r[C1,O_w]$. R_X and R_Y were increased in steps of 0.2 Å with harmonic restraints of 5000 kcal/mol•Å^2. Geometrical optimisation of the structures was performed at each point until the gradient was less than 0.01 kcal/(mol•Å). The energy was then computed by a single-point calculation, which removed the energy contribution due to reaction coordinate restraints.

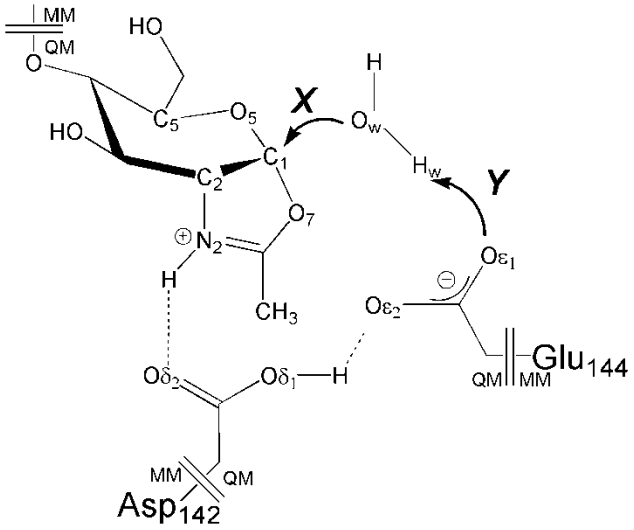

Figure 1. QM regions used in this study showing two individual steps for the deglycosylation by *S. marcescens* ChiB (***X*** and ***Y*** represent the nucleophilic attack of catalytic water and proton abstraction respectively)

RESULTS AND DISCUSSION

Structure of ChiB-Intermediate Complex

The model of ChiB-intermediate complex is quite stable during the QM/MM MD simulation, as demonstrated by the root mean square deviation (RMSD) of about 0.44 ± 0.07 Å in Figure 2. Table 1 lists some important geometric parameters from the X-ray experiment, QM/MM MD simulation and QM/MM minimisation. As can be seen, the geometry from our simulation is in good agreement with the X-ray structure. Tyr214 and Asp142 show very stable H-bonds (s.d. = 0.22 and 0.11 Å respectively) during the QM/MM MD simulation (Table 1), indicating the importance of these two residues in stabilising the intermediate (oxazolinium ion). Importantly, the torsional angle (C2–C1–O5–C5) representing the chair conformation of the oxazolinium ion ring is very stable during the simulation, which is in excellent agreement with the X-ray experiment, indicating the suitability of the AM1 method in representing the conformation of the putative oxazolinium ion ring. Although the simulated distances of C1–O_w and Asp142:Oδ1–Oε2:Glu144 seem to be greater than those from experiment, they were found to improve during the restrained QM/MM minimisation as shown in Table 1, giving a reasonable starting point for subsequent reaction path calculation.

Maejo Int. J. Sci. Technol. **2011**, *5*(01), 47-57

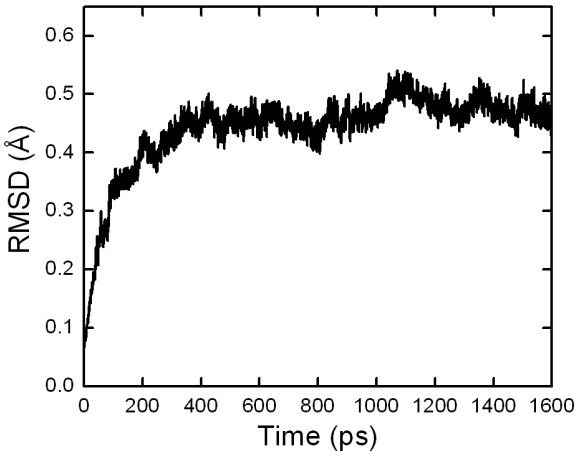

Figure 2. Root mean square displacement (RMSD) of the heavy atoms of ChiB-intermediate complex during 1.6 ns of QM/MM MD simulation

Table 1. Some important geometric parameters obtained from X-ray experiment, simulation (QM/MM MD) and minimisation (QM/MM)

Geometric parameter [a,b]	Experiment [c]	Simulation	Minimisation
C1–O_w	2.75	3.40 ± 0.50	2.76
Glu144:Oε_1–O_w	2.67	2.96 ± 0.51	2.54
Asp142:Oδ_1–Oε_2:Glu144	2.26	3.70 ± 0.55	3.04
N2–Oδ_2:Asp142	2.92	2.88 ± 0.11	2.78
Tyr214: OH–O7	3.05	3.10 ± 0.22	3.12
O_w–C1–O7	152.6	165.8 ± 8.8	146.2
C2–C1–O5–C5	–43.5	–43.5 ± 6.1	–44.2

[a]Atomic numbering corresponds to Figure 1, whereas other atom types follow the CHARMM format.

[b] Distances are given in angstroms; angles (bond angle and torsional angle) are given in degrees.

[c] from X-ray crystal structure (PDB code 1E6Z) [6]

Reaction Path

Figure 3 shows the AM1/CHARMM22 potential energy surface (PES) describing two key events (***X*** and ***Y*** in Figure 1): the nucleophilic attack of oxygen (O_w) of catalytic water at the C1 anomeric carbon (R_X) and the proton (H_w) abstraction from water molecule by oxygen atom (Oε_1) of the deprotonating Glu144 (R_Y). The stationary points for minima and saddle points located on the PES are also depicted.

As indicated in Figure 3, the PES clearly shows the presence of two transition states (TS1 and TS2) indicating a stepwise mechanism in which the nucleophilic attack occurs as the first step followed by the proton abstraction. This observation is unexpected as the deglycosylation reaction

Maejo Int. J. Sci. Technol. **2011**, *5*(01), 47-57

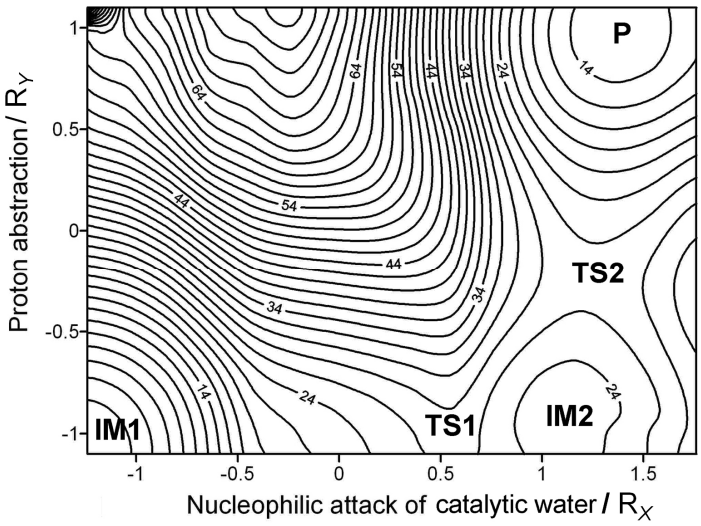

Figure 3. AM1/CHARMM22 potential energy surface for the deglycosylation reaction catalysed by *S. marcescens* ChiB [IM1 = oxazolinium intermediate 1; TS1 = transition state 1; IM2 = intermediate 2; TS2 = transition state 2; P = dimer product (NAG_2)]. The unit of QM/MM energies is in kcal/mol.

has been proposed to occur via only one transition state as well as the glycosylation [6]. This findings have suggested a new mechanism for the deglycosylation by *S. marcescens* ChiB. The changes of the QM/MM energy for IM1 → TS1 and IM2 → TS2 are 26.8 and 4.0 kcal/mol respectively (Table 2), indicating that the rate-limiting step for the deglycosylation reaction is the nucleophilic attack by catalytic water. The calculated barrier of about 27 kcal/mol is considerably higher than the experimentally determined barrier of 16.1 kcal/mol estimated from the experimental rate constant of 40.9 s^{-1} at 310 K [23] using transition state theory [24]. It should be noted, however, that such experimental barrier was estimated based on the overall reaction (i.e. glycosylation and deglycosylation). Therefore, although a high value of calculated barrier is observed in this study, an accurate energy barrier is not expected. More importantly, as no clear evidence on the presence of a rate-determining step in ChiB-assisted reactions has been reported previously, new insight into the catalytic mechanism of the deglycosylation by *S. marcescens* ChiB at molecular level has thus been gained.

The stabilisation energy of the reactive site (QM region) provided by the protein environment (MM region) along the stationary points has also been analysed relative to the energy in IM1. The result indicates that the influence of the protein environment on the stabilisation of the reactive site gradually decreases, as reflected by the negative values of stabilisation energy (Table 2), which provides evidence that the intermediate state (IM1) is central to the catalysis by ChiB.

Geometry along the Reaction Path

Snapshots of stationary structures (IM1, TS1, IM2, TS2, and P) and their corresponding geometric parameters along the deglycosylation path are shown in Figure 4 and Table 2 respectively. The starting structure of the ground state of ChiB-intermediate (IM1) indicates a suitable

Maejo Int. J. Sci. Technol. **2011**, *5*(01), 47-57

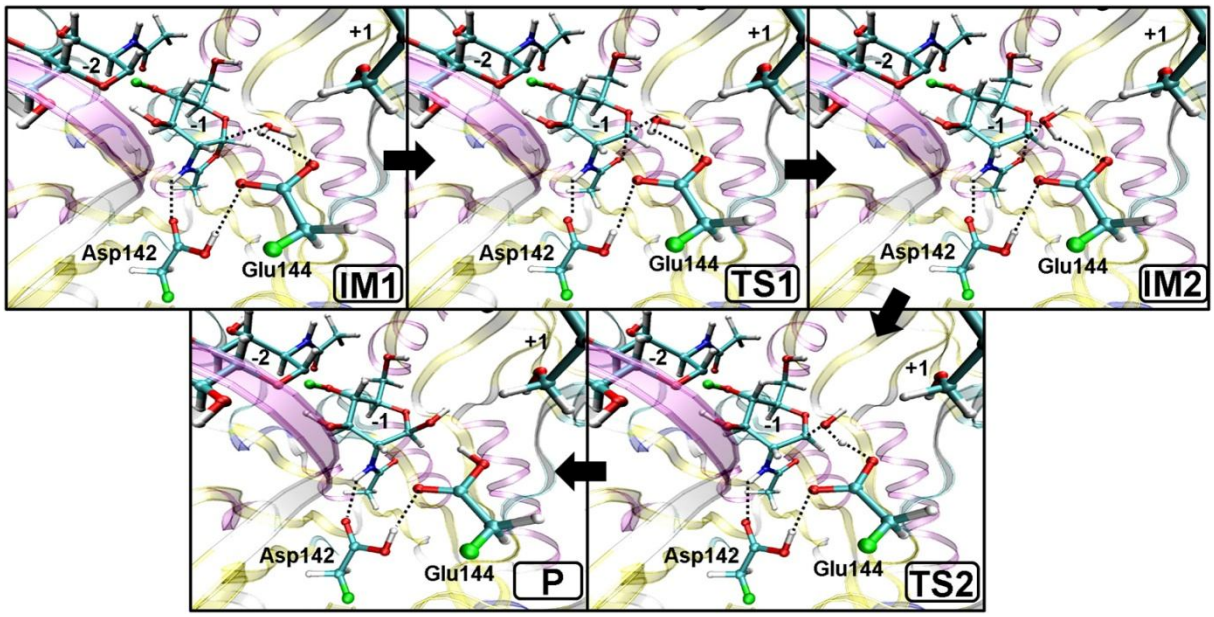

Figure 4. Snapshots of the stationary structures along the deglycosylation path

Table 2. Relevant geometric parameters and energy values of different stationary structures on the PES calculated at AM1/CHARMM22 level

Parameter [a]	IM1	TS1	IM2	TS2	P
C1–O_w	2.73	1.96	1.53	1.50	1.43
C1–O7	1.49	2.52	2.69	2.66	2.79
C1–O5	1.39	1.32	1.38	1.39	1.41
O_w–H_w	0.97	0.98	1.02	1.15	2.00
Glu144:Oε_1–H_w	2.07(2.56)[b]	2.09	1.92	1.35	1.00
Asp142:Hδ_1–Oε_2:Glu144	2.70(3.64)[b]	2.82	2.78	2.29	2.48
HN2–Oδ_2:Asp142	2.09(2.83)[b]	2.13	2.13	2.13	2.21
O_w–C1–O7	147.7	150.8	159.1	156.6	151.8
C2–C1–O5–C5	–27.8	–11.1	5.1	1.6	0.4
QM/MM energy	0	26.8	22.7	26.7	12.3
Stabilisation energy [c]	0	–22.6	–27.1	–48.9	–71.4

[a] Distances are given in angstroms; angles (bond angle and torsional angle) are given in degrees; and energies are given in kcal/mol.
[b] Heavy atom distance
[c] Stabilisation energy is the energy difference between full QM/MM system and only QM atoms relative to that of IM1.

Maejo Int. J. Sci. Technol. **2011**, *5*(01), 47-57

position for nucleophilic attack of water molecule as evidenced by the distances of C1–O_w (2.73 Å) and Glu144:Oε_1–H_w (2.07 Å) and the O_w–C1–O7 angle (147.7º), which is in good accordance with the X-ray structure shown in Table 1. It is also observed from the X-ray experiment [6] that the chair conformation of the oxazolinium ring is distorted by only about 15º, indicating a relaxed conformation of the ring in the beginning of the nucleophilic reaction.

In TS1, the water molecule makes an attack at the anomeric centre (C1) to some extent (Table 2), which is close enough to break the oxazolinium ring by lengthening the C1-O7 distance ~1.0 Å from the IM1. At the same time, the chair conformation of the oxazolinium ring is distorted to a half-chair, as shown by a more planar conformation around the C1–O5 bond (C2–C1–O5–C5 = –11º). Such planarity, together with a shortening C1–O5 bond to a partial double bond (1.39 Å at IM1 to 1.32 Å at TS1), indicates the formation of an oxocarbenium-like ion. Note that this half-chair conformation is found to remain until the product state but with increasing trend of planarity (see C2–C1–O5–C5 in Table 2). The Glu144:Oε_1–H_w distance does not change much at this stage, suggesting that no proton abstraction occurs here.

In IM2, as can be seen in Figure 4, the water molecule orients itself to be poised for in-line attack at the anomeric C1 atom as shown by the largest O_w–C1–O7 angle (~160º) and to facilitate the proton abstraction, which initially happens in this stage, as indicated by a slight change in the O_w–H_w distance (0.98 Å at TS1 to 1.02 Å at IM2) and the Glu144:Oε_1–H_w distance (2.09 Å at TS1 to 1.92 Å at IM2). Meanwhile, the oxygen atom of catalytic water moves closer to the anomeric centre (1.96 Å in TS1 to 1.53 Å in IM2) and again the increasing C1–O7 distance (2.52 Å in TS1 to 2.69 Å in IM2) is also observed.

In TS2, the proton abstraction from the water molecule to Glu144 is almost complete at this stage (Figure 4): the distance of the moving proton to the oxygen of Glu144 (Oε_1–H_w) is 1.15 Å, whereas the distance to the water oxygen (O_w–H_w) is 1.35 Å. During the proton abstraction, Glu144 is stabilised by the hydrogen atom from Asp142 as indicated by a large decrease in the Hδ□–Oε2 distance (2.78 Å at IM2 to 2.29 Å at TS2).

In the product (P), the proton abstraction is complete after Glu144 accepts the hydrogen atom (H_w) from the deprotonated water, resulting in the expulsion of the 2-acetamido group from the anomeric C1 carbon (2.66 Å at TS2 to 2.79 Å at P). This yields the sugar hemiacetal product with overall retention of stereochemistry. The releasing of a dimeric sugar product (NAG at subsite –1, –2, as shown in Figure 4) may be indicated by elongation of the H-bond distance of HN2–Oδ_2:Asp142 from 2.13 Å to 2.21 Å (Table 2).

CONCLUSIONS

In this study, the deglycosylation step of chitin hydrolysis catalysed by *S. marcescens* ChiB was investigated by hybrid QM/MM calculation based on the available crystal structure of ChiB. The QM/MM PES calculated at AM1/CHARMM22 level was carried out using adiabatic mapping to track the possible reaction pathway and locate and characterise the structures corresponding to the stationary points. The PES showed the presence of two transition states, indicating that the deglycosylation path follows a stepwise mechanism in which the nucleophilic attack of water at the anomeric carbon occurs as the first step, followed by proton abstraction from water molecule to the

oxygen atom of Glu144. These results differ from the current belief that the deglycosylation should occur via a single transition state. The calculated barriers for the two transition states suggest that the nucleophilic attack of water molecule is the rate-limiting step for the deglycosylation. In addition, an oxocarbenium-like character in the first transition state was also captured. Such ionic character, as suggested by our QM/MM study, is likely to occur in both glycosylation and deglycosylation by ChiB, which seems to support previous findings that the formation of an oxocarbenium ion is a major characteristic of the hydrolysis of the β-glycosidic linkage.

ACKNOWLEDGEMENTS

The Office of the Higher Education Commission (CHE), Thailand is thanked for a grant under the Strategic Scholarships for Frontier Research Network for the Joint PhD Program (Grant No. CHE-PhD-SW/54/2549) for J. J. The Centre for Innovation in Chemistry (PERCH-CIC) and the Graduate School of Chiang Mai University are also thanked for the partial financial support. Engineering and Physical Sciences Research Council (EPSRC) and Biotechnology and Biological Sciences Research Council are thanked for support for A. J. M.

REFERENCES

1. B. Henrissat, "A classification of glycosyl hydrolases based on amino acid sequence similarities", *Biochem. J.*, **1991**, *280*, 309-316.
2. G. Davies and B. Henrissat, "Structures and mechanisms of glycosyl hydrolases", *Structure*, **1995**, *3*, 853-859.
3. O. A. Andersen, M. J. Dixon, I. M. Eggleston and D. M. F. van Aalten, "Natural product family 18 chitinase inhibitors", *Nat. Prod. Rep.*, **2005**, *22*, 563-579.
4. B. Synstad, S. Gaseidnes, D. M. F. van Aalten, G. Vriend, J. E. Nielsen and V. G. H. Eijsink, "Mutational and computational analysis of the role of conserved residues in the active site of a family 18 chitinase", *Eur. J. Biochem.*, **2004**, *271*, 253-262.
5. I. Tews, A. C. T. van Scheltinga, A. Perrakis, K. S. Wilson and B. W. Dijkstra, "Substrate-assisted catalysis unifies two families of chitinolytic enzymes", *J. Am. Chem. Soc.*, **1997**, *119*, 7954-7959.
6. D. M. F. van Aalten, D. Komander, B. Synstad, S. Gaseidnes, M. G. Peter and V. G. H. Eijsink, "Structural insights into the catalytic mechanism of a family 18 exo-chitinase", *Proc. Natl. Acad. Sci. USA*, **2001**, *98*, 8979-8984.
7. G. Vaaje-Kolstad, D. R. Houston, F. V. Rao, M. G. Peter, B. Synstad, D. M. F. van Aalten and V. G. H. Eijsink, "Structure of the D142N mutant of the family 18 chitinase ChiB from *Serratia marcescens* and its complex with allosamidin", *Biochim. Biophys. Acta*, **2004**, *1696*, 103-111.
8. N. Cetinbas, M. S. Macauley, K. A. Stubbs, R. Drapala and D. J. Vocadlo, "Identification of Asp174 and Asp175 as the key catalytic residues of human O-GlcNAcase by functional analysis of site-directed mutants", *Biochem.*, **2006**, *45*, 3835-3844.

9. A. Warshel and M. Levitt, "Theoretical studies of enzymic reactions: dielectric, electrostatic and steric stabilization of the carbonium ion in the reaction of lysozyme", *J. Mol. Biol.*, **1976**, *103*, 227-249.
10. H. M. Senn and W. Thiel, "QM/MM methods for biomolecular systems", *Angew. Chem. Int. Ed. Engl.*, **2009**, *48*, 1198-1229.
11. K. E. Ranaghan and A. J. Mulholland, "Investigations of enzyme-catalysed reactions with combined quantum mechanics/molecular mechanics (QM/MM) methods", *Int. Rev. Phys. Chem.*, **2010**, *29*, 65-133.
12. A. L. Bowman, I. M. Grant and A. J. Mulholland, "QM/MM simulations predict a covalent intermediate in the hen egg white lysozyme reaction with its natural substrate", *Chem. Commun.*, **2008**, 4425-4427.
13. L. Petersen, A. Ardevol, C. Rovira and P. J. Reilly, "Mechanism of cellulose hydrolysis by inverting GH8 endoglucanases: a QM/MM metadynamics study", *J. Phys. Chem. B*, **2009**, *113*, 7331-7339.
14. N. F. Bras, P. A. Fernandes and M. J. Ramos, "QM/MM studies on the β-galactosidase catalytic mechanism: Hydrolysis and transglycosylation reactions", *J. Chem. Theory Comput.*, **2010**, *6*, 421-433.
15. J. Liu, X. Wang and D. Xu, "QM/MM study on the catalytic mechanism of cellulose hydrolysis catalyzed by cellulase Cel5A from Acidothermus cellulolyticus", *J. Phys. Chem. B*, **2010**, *114*, 1462-1470.
16. L. Petersen, A. Ardevol, C. Rovira and P. J. Reilly, "Molecular mechanism of the glycosylation step catalyzed by Golgi α-mannosidase II: a QM/MM metadynamics investigation", *J. Am. Chem. Soc.*, **2010**, *132*, 8291-8300.
17. J. Jitonnom, V. S. Lee, P. Nimmanpipug, H. A. Rowlands and A. J. Mulholland, *Unpublished results*.
18. B. R. Brooks, R. E. Bruccoleri, B. D. Olafson, D. J. States, S. Swaminathan and M. Karplus, "CHARMM: A program for macromolecular energy, minimization and dynamics calculations", *J. Comp. Chem.*, **1983**, *4*, 187-217.
19. M. J. S. Dewar, E. G. Zoebisch, E. F. Healy and J. J. P. Stewart, "AM1: A new general purpose quantum mechanical molecular model", *J. Am. Chem. Soc.*, **1985**, *107*, 3902-3909.
20. A. D. MacKerell, Jr., D. Bashford, M. Bellott, R. L. Dunbrack, J. D. Evanseck, M. J. Field, S. Fischer, J. Gao, H. Guo, S. Ha, D. Joseph-McCarthy, L. Kuchnir, K. Kuczera, F. T. K. Lau, C. Mattos, S. Michnick, T. Ngo, D. T. Nguyen, B. Prodhom, W. E. III Reiher, B. Roux, M. Schlenkrich, J. C. Smith, R. Stote, J. Straub, M. Watanabe, J. Wiorkiewicz-Kuczera, D. Yin and M. Karplus, "All-atom empirical potential for molecular modeling and dynamics studies of proteins", *J. Phys. Chem. B*, **1998**, *102*, 3586-3616.
21. C. L. Brooks and M. Karplus, "Deformable stochastic boundaries in molecular dynamics", *J. Chem. Phys.*, **1983**, *79*, 6312-6325.
22. A. Lodola, M. Mor, J. C. Hermann, G. Tarzia, D. Piomelli and A. J. Mulholland, "QM/MM modelling of oleamide hydrolysis in fatty acid amide hydrolase (FAAH) reveals a new mechanism of nucleophile activation", *Chem. Commun.*, **2005**, 4399-4401.

Maejo Int. J. Sci. Technol. **2011**, *5*(01), 47-57

23. I. M. Krokeide, B. Synstad, S. Gaseidne, S. J. Horn, V. G. H. Eijsink and M. Sorlie, "Natural substrate assay for chitinases using high-performance liquid chromatography: a comparison with existing assays", *Anal. Biochem.*, **2007**, *363*, 128-134.
24. M. Garcia-Viloca, J. Gao, M. Karplus and D. G. Truhlar, "How enzymes work: Analysis by modern rate theory and computer simulations", *Science*, **2004**, *303*, 186-195.